

Crystal growth of metastable rutile-type $\text{Ti}_x\text{Sn}_{1-x}\text{O}_2$ solid solutions in an aqueous system

Hiroaki Uchiyama and Hiroaki Imai*

Received (in Cambridge, UK) 8th August 2005, Accepted 14th October 2005

First published as an Advance Article on the web 7th November 2005

DOI: 10.1039/b511223k

Nanoscale grains of crystalline $\text{Ti}_x\text{Sn}_{1-x}\text{O}_2$ were directly grown over the whole range of $[\text{Ti}]/([\text{Ti}] + [\text{Sn}])$ ratio ($x = 0.00\text{--}1.00$) in aqueous solutions at near room temperature.

Transparent semiconducting oxides that have a wide band-gap, such as titanium dioxide (TiO_2) and tin dioxide (SnO_2), attract much attention because of their specific electronic and optical properties.^{1–16} Recently, anatase-type TiO_2 , which exhibits a high photocatalytic activity,¹³ has been widely studied for applications in many fields, including microorganism photolysis,¹⁴ medical treatment¹⁵ and environmental purification.¹⁶ On the other hand, rutile-type TiO_2 , known as a white pigment, has not been utilized in functional devices because of its low photocatalytic activity, originating from a low mobility of carriers. Since rutile-type SnO_2 has high transparency, high mobility of electrons, and high sensitivity for reducing gas molecules, thin films and powders of SnO_2 have been extensively applied to transparent electrodes^{17,18} and gas sensors.¹⁹ The electron mobility in SnO_2 is two orders of magnitude larger than that in TiO_2 ,¹¹ whereas both oxides have the same lattice structure. Consequently, solid solutions denoted by $\text{Ti}_x\text{Sn}_{1-x}\text{O}_2$ are expected to exhibit a specific performance as a new type of functional materials.^{2,6–9,11,12} Although the solid solutions are formed over the whole range of the $[\text{Ti}]/([\text{Ti}] + [\text{Sn}])$ ratio ($x = 0.00\text{--}1.00$) over 1500 °C, only TiO_2 -rich ($x < 0.1$) and SnO_2 -rich ($x > 0.9$) phases are thermodynamically stable at room temperature.²⁰ Several studies about the preparation of the solid solutions have been reported using sol–gel^{2,7,11} and co-precipitation methods,^{6,21} however, the control of the composition of rutile-type $\text{Ti}_x\text{Sn}_{1-x}\text{O}_2$ in the whole range of the molar ratio has not been achieved.

In recent years, the preparation of functional metal oxides from aqueous solution has received much attention in regard to low-energy and environmentally benign processes.^{22,23} The morphology at the nanometer level and the compositions including organic and inorganic components have been reported to be controlled in the solution routes. Moreover, the direct deposition of crystals in aqueous solutions would be useful for the preparation of thermodynamically metastable structures because heat treatments for the crystallization are not required. Here, we pay attention to the similarity between the deposition conditions of TiO_2 and SnO_2 to prepare rutile-type solid solutions of TiO_2 and SnO_2 in an aqueous system.^{22,23} Consequently, the direct growth of crystalline $\text{Ti}_x\text{Sn}_{1-x}\text{O}_2$ solid solutions at near room temperature

was successful by adjusting the pH and concentrations of the raw materials. The $[\text{Ti}]/([\text{Ti}] + [\text{Sn}])$ ratio of the solid solutions prepared in this work could be varied over the whole range ($x = 0.00\text{--}1.00$). We discuss how the structures and properties of the solid solutions depend on the $[\text{Ti}]/([\text{Ti}] + [\text{Sn}])$ ratio.

Precursor solutions were obtained by dissolving $\text{TiOSO}_4 \cdot x(\text{H}_2\text{O})$ ($x_{\text{ave}} = 4.6$) and SnF_2 into an HCl aqueous solvent at pH 0.6 with stirring for 1 h at room temperature. The total concentration of the metal ions ($[\text{Ti(IV)}] + [\text{Sn(II)}]$) was adjusted to 0.01 M. Deposition was performed in the solutions by being kept at 60 °C from several hours to several days in an electric oven. The precipitates were obtained after centrifuging and drying at 60 °C for 1 day. The samples were calcined at 200–700 °C in air.

The morphology of the particles was observed with a field emission scanning electron microscope (FESEM, Hitachi S-4700) with 5 kV accelerating voltage. The specific surface area was calculated by BET methods using nitrogen adsorption isotherms obtained at 77 K with a Micromeritics TriStar 3000. X-Ray diffraction (XRD) patterns were recorded with a Rigaku RAD-C system with Cu K α radiation. Diffuse reflection spectra (DRS) of a powdery sample were measured in the range of 200–600 nm with a JASCO UV-vis spectrophotometer V-560 with MgO as a reference sample. Energy dispersive X-ray analysis (EDX) was measured with an EDAX GENESIS 2000 on a scanning electron microscope (Hitachi S-3150). The photocatalytic activity was evaluated by the decomposition of methylene blue (MB) in water under illumination from a conventional black light (6 W \times 2, 0.1 mW cm⁻²) with 0.1 g powders deposited in an open container of 30 cm³ in volume. The variation of the MB concentration was monitored with a specific absorption band at 665 nm using a Shimadzu UV2500 UV-vis spectrometer.

Fig. 1 shows SEM images and specific surface areas of the precipitates prepared at various molar ratios of TiO_2 and SnO_2 . The products had a porous structure consisting of nanoscale grains and exhibiting large specific surface areas above 100 m² g⁻¹.

Fig. 2 illustrates the relationship between the concentration ratio of $[\text{Ti(IV)}]/([\text{Ti(IV)}] + [\text{Sn(II)}])$ in precursor solutions (defined as x) and the ratio of $[\text{Ti}]/([\text{Ti}] + [\text{Sn}])$ in the products estimated with EDX (defined as x'). The composition of the products was almost the same as that of the precursor solutions, although the amount of TiO_2 slightly decreased at $x = 0.5\text{--}0.8$.

The XRD patterns, as shown in Fig. 3, indicate that all of the as-deposited products were assigned to a single phase of the rutile-type structure. Diffraction peaks assigned to the rutile structure shifted between those corresponding to pure TiO_2 and pure SnO_2 with the variation of the composition. The crystalline solid solutions were formed in thermodynamically metastable

H. Uchiyama, Prof. H. Imai, Department of Applied Chemistry, Faculty of Science and Technology, Keio University, 3-14-1 Hiyoshi, Kohoku-ku, Yokohama 223-8522, Japan. E-mail: hiroaki@applied.keio.ac.jp; Fax: +81-45-566-1551

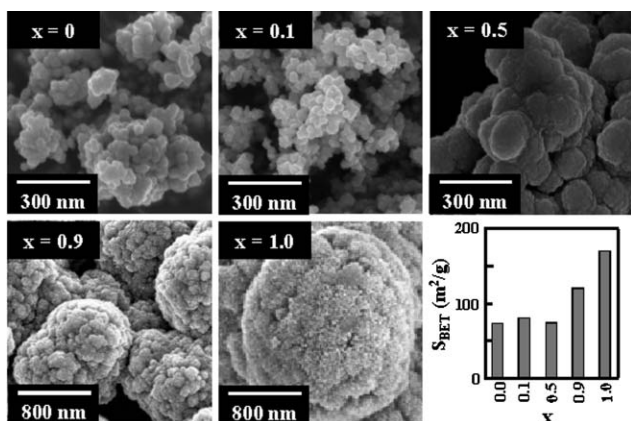


Fig. 1 SEM images and the specific surface area of the solid solutions ($x = 0.0$ – 1.0).

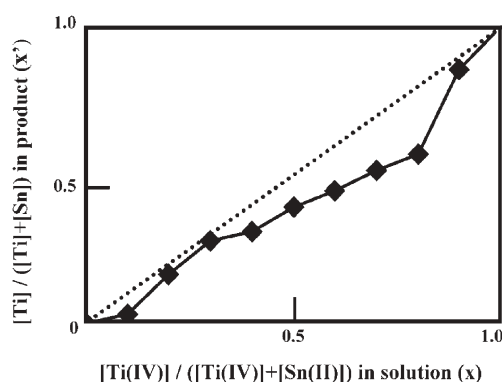


Fig. 2 Relationship of the components between the precursor solutions and the products estimated with EDX.

compositions ($x = 0.1$ – 0.9), which indicates that solid solutions of $\text{Ti}_x\text{Sn}_{1-x}\text{O}_2$ were obtained in all the ratios of $[\text{Ti}]/([\text{Ti}] + [\text{Sn}])$ ($x = 0.00$ – 1.00).

Fig. 4 shows that the lattice parameters estimated from the XRD patterns were continuously varied as a function of the composition. We found that $a(a_1)$ was not equal to $b(a_2)$ in the rutile structure of the products. This fact indicates the deformation of the lattice of the as-deposited solid solutions. The strain of the lattice was eliminated by calcination at a temperature over $200\text{ }^\circ\text{C}$. Although the same behavior on the rutile-type solid solutions has already reported by Cassia-Santos *et al.*,²¹ we observed the lattice relaxation in the whole range of the composition including metastable $\text{Ti}_x\text{Sn}_{1-x}\text{O}_2$ ($0.1 < x < 0.9$).

Moreover, the phase separation of the metastable phase was not observed even by calcination at $700\text{ }^\circ\text{C}$ in our work. The heat treatment was also effective for the elimination of impurities, such as sulfate and fluoride ions, remaining on the surface of the products.

Fig. 5 shows the diffuse reflection spectra and band-gap energies calculated from the adsorption edges of the solid solutions. The adsorption edge of the solid solution shifted between that of pure SnO_2 ($x' = 0.0$) and pure TiO_2 ($x' = 1.0$) with variation of the composition of the products. An adsorption tail for pure SnO_2 is ascribed to the presence of Sn(II) .²⁴ On the other hand, additional adsorption caused by the presence of impurities of the crystal

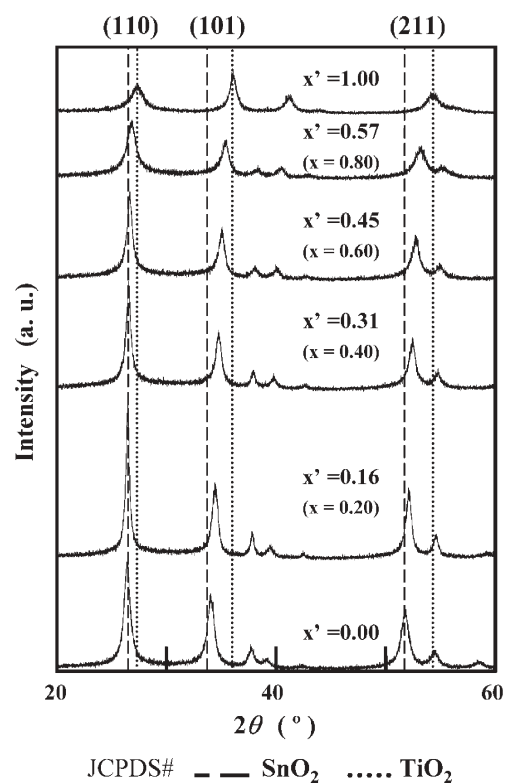


Fig. 3 XRD patterns of $\text{Ti}_x\text{Sn}_{1-x}\text{O}_2$ solid solution samples ($x' = 0.0$ – 1.0).

structures was not detected in solid solutions containing TiO_2 . The band-gap energies of the solid solutions continuously varied in proportion to the composition, indicating that the band structure of the semiconducting oxides was controllable by substitution of the cations. The adsorption peaks were not separated by calcination, as mentioned above in XRD.

These products of solid solutions are advantageous for catalytic applications because of their high specific surface area. The photocatalytic activity of the solid solutions was investigated using products calcined at $400\text{ }^\circ\text{C}$ because the strain in the lattice of the rutile structure was annealed and a decrease in the specific surface area due to sintering was not observed at that temperature.

Fig. 6 shows the decomposition rate of MB by the photocatalytic reaction under illumination from a black light. The activity of the SnO_2 -rich solid solutions ($x = 0.00$ – 0.30) was not observed because of low absorbability of the products in the UV region emitted from the black light (300 – 400 nm). On the other hand, the TiO_2 -rich solid solution was found to exhibit a sufficient photocatalytic performance. In particular, the sample of $x = 0.90$ ($x' = 0.85$) had a photocatalytic activity higher than that of pure rutile TiO_2 ($x = 1.00$) and commercially available anatase powder with large surface area of *ca.* $300\text{ m}^2\text{ g}^{-1}$ (Ishihara ST-01).

In summary, we successfully prepared nanoscale grains of rutile-type $\text{Ti}_x\text{Sn}_{1-x}\text{O}_2$ in an aqueous system at near room temperature, and achieved the control of the composition of the solid solutions in the whole range ($x = 0.0$ – 1.0). The band-gap of the crystalline solid solutions was continuously varied with the lattice parameters of the rutile structures. The control of the band gap and the electronic properties of the semiconducting transparent oxide materials would provide the possibility of new functions and high performance.

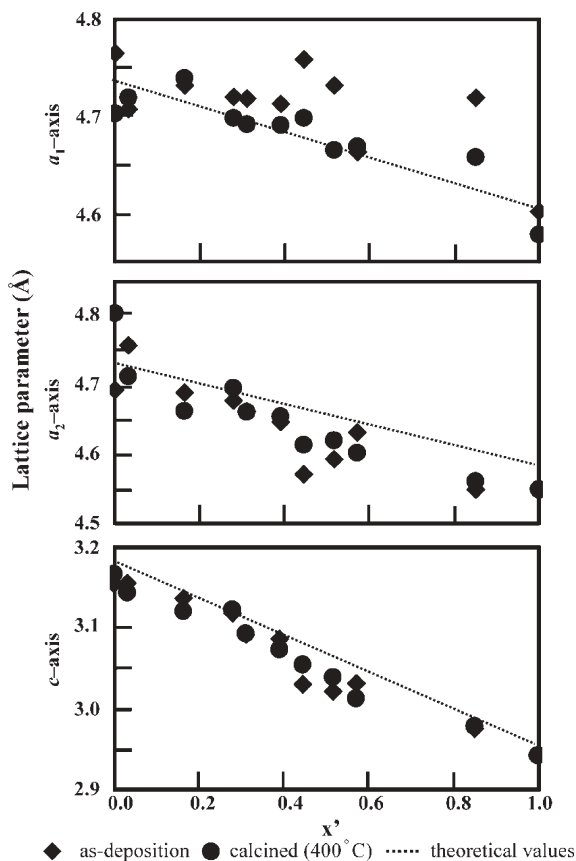


Fig. 4 Relationship between the lattice parameters a_1 , a_2 , c and the component of $\text{Ti}_x\text{Sn}_{1-x}\text{O}_2$ solid solutions.

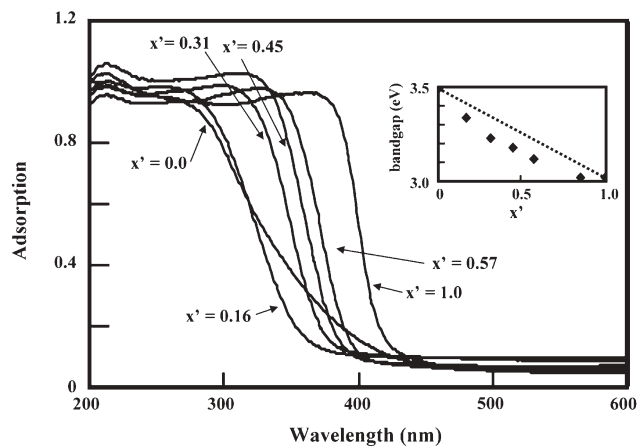


Fig. 5 Diffuse reflection spectra and bandgap energies of $\text{Ti}_x\text{Sn}_{1-x}\text{O}_2$ solid solution ($x' = 0.0$ – 1.0).

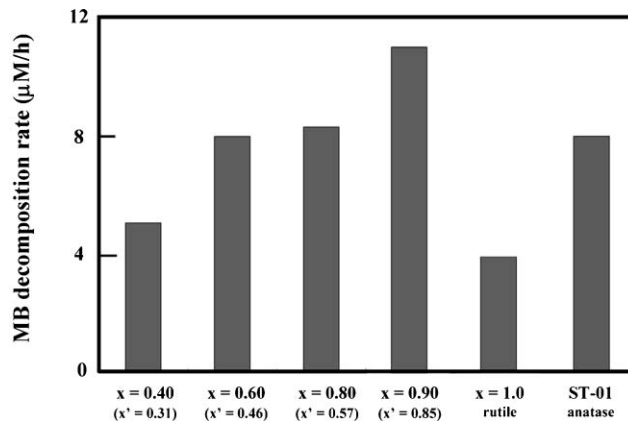


Fig. 6 Decomposition rate of MB with $\text{Ti}_x\text{Sn}_{1-x}\text{O}_2$ solid solutions ($x = 0.0$ – 1.0).

Notes and references

- I. Bedja and P. V. Kamat, *J. Phys. Chem.*, 1995, **99**, 9182.
- Y. Cao, Y. M. Zhou, Y. Shan, H. X. Ju, X. J. Xue and Z. H. Wu, *Adv. Mater.*, 2004, **16**, 1189.
- Y. A. Cao, W. S. Yang, W. F. Zhang, G. Z. Liu and P. L. Yue, *New J. Chem.*, 2004, **28**, 218.
- W. Y. Chung, D. D. Lee and B. K. Sohn, *Thin Solid Films*, 1992, **221**, 304.
- S. Komornicki, M. Radecka and M. Rekas, *J. Mater. Sci.*, 2001, **12**, 11.
- J. Lin, J. C. Yu, D. Lo and S. K. Lam, *J. Catal.*, 1999, **183**, 368.
- M. M. Oliveira, D. C. Schnitzler and A. J. G. Zarbin, *Chem. Mater.*, 2003, **15**, 1903.
- M. Radecka, P. Pasierb, K. Zakrzewska and M. Rekas, *Solid State Ionics*, 1999, **119**, 43.
- M. Radecka, K. Zakrzewska and M. Rekas, *Sens. Actuators, B*, 1998, **47**, 194.
- J. Yang, D. Li, X. Wang, X. J. Yang and L. D. Lu, *J. Solid State Chem.*, 2002, **165**, 193.
- K. Zakrzewska, *Thin Solid Films*, 2001, **391**, 229.
- Z. L. Zhang, M. Jun and X. Y. Yang, *Chem. Eng. J.*, 2003, **95**, 15.
- A. Fujishima and K. Honda, *Nature*, 1972, **238**, 37.
- K. Sunada, Y. Kikuchi, K. Hashimoto and A. Fujishima, *Environ. Sci. Technol.*, 1998, **32**, 726.
- R. X. Cai, Y. Kubota, T. Shuin, H. Sakai, K. Hashimoto and A. Fujishima, *Cancer Res.*, 1992, **52**, 2346.
- M. R. Hoffmann, S. T. Martin, W. Y. Choi and D. W. Bahnemann, *Chem. Rev.*, 1995, **95**, 69.
- R. E. Presley, C. L. Munsee, C. H. Park, D. Hong, J. F. Wager and D. A. Keszler, *J. Phys. D: Appl. Phys.*, 2004, **37**, 2810.
- A. P. Rizzato, C. V. Santilli, S. H. Pulcinelli, Y. Messaddeq and P. Hammer, *J. Sol-Gel Sci. Technol.*, 2004, **32**, 155.
- Y. L. Wang, X. C. Jiang and Y. N. Xia, *J. Am. Chem. Soc.*, 2003, **125**, 16176.
- H. P. Naidu and A. V. Virkar, *J. Am. Ceram. Soc.*, 1998, **81**, 2176.
- M. R. Cassia-Santos, A. G. Souza, L. E. B. Soledade, J. A. Varela and E. Longo, *J. Therm. Anal. Calorim.*, 2005, **79**, 415.
- H. Ohgi, T. Maeda, E. Hosono, S. Fujihara and H. Imai, *Cryst. Growth Des.*, 2005, **5**, 1079.
- S. Yamabi and H. Imai, *Chem. Mater.*, 2002, **14**, 609.
- H. M. Deng and J. M. Hossenlopp, *J. Phys. Chem. B*, 2005, **109**, 66.